Micron 44 (2013) 185–192

Contents lists available at SciVerse ScienceDirect

Micron

journal homepage: www.elsevier.com/locate/micron

A high resolution analysis of the structure and chemical composition of the calcareous corpuscles from *Mesocestoides corti*

Cora Chalar[a], Murielle Salomé[b], Mario Señorale-Pose[a], Mónica Marín[a], C. Terry Williams[c], Yannicke Dauphin[d,*]

[a] *Sección Bioquímica, Facultad de Ciencias, Universidad de la República, Iguá 4225, CP 11400, Montevideo, Uruguay*
[b] *ID21, European Synchrotron Radiation Facility, 6, Rue Horowitz, BP 220, 38043 Grenoble, France*
[c] *Department of Mineralogy, Natural History Museum, Cromwell Road, London SW7 5BD, United Kingdom*
[d] *Micropaléontologie, UFR TEB, Case 104, Université Paris VI, 4 Place Jussieu, 75252 Paris Cedex 05, France*

ARTICLE INFO

Article history:
Received 29 January 2012
Received in revised form 15 June 2012
Accepted 16 June 2012

Keywords:
Calcareous corpuscles
Cestodes
Biomineralization
Nanostructure
Chemical composition

ABSTRACT

Mesocestoides corti (syn. vogae), similar to many other cestode platyhelminthes, contains abundant calcium carbonate structures called calcareous corpuscles. These concretions that may constitute as much as 40% of the dry weight of the body, and were proposed to form intracellularly in certain parenchymal cells. As an approach to elucidate the biological role of calcareous corpuscles in cestodes, our aim was to characterize more precisely the structure and topological composition of the corpuscles from *M. corti*. Employing a variety of high resolution technical approaches, we found that the calcareous corpuscles are spheroid or ovoid layered concretions. They are formed by topographically homogeneous but compositionally heterogeneous layers, suggesting a cyclic process of biomineralization. The layers are composite structures, with granules of tens of nanometers, each surrounded by a cortex of about eight nanometers.

1. Introduction

Biomineralization is a widespread phenomenon among invertebrates. Molluscs, echinoderms and crustaceans contain mineralized compounds that perform functions ranging from the support to protective covers. Some of their representatives have been useful models helping to define the concept of biologically controlled mineralization. Calcium carbonate is one of the most abundant biominerals and is the most often found in invertebrate organisms (Lowenstam, 1981; Wilt et al., 2003).

Cestodes, parasitic organisms belonging to the phylum Platyhelminthes, produce mineral concretions that are known as calcareous corpuscles (CCs). The function of CCs is a matter of speculation, and several hypotheses have been proposed (von Brand et al., 1965a,b; Etges and Marinakis, 1991; Smyth, 1969). The size and number of CC varies among different species, but in all cases CCs represent a percentage of not less than 10% of the dry weight of the body (McCullough and Fairweather, 1987).

Unlike most of invertebrate organisms, the mineralization in cestodes is an intracellular process. Nevertheless for many of them, the nature of the cells involved in the formation of CC is controversial. Similarly, the mechanism for the biocomposite formation is still poorly understood (Vargas-Parada and Laclette, 1999).

The available information on elemental composition of the CCs shows the presence of Ca, Mg, phosphate and carbonate, and traces of a variety of elements such as Al, Cr, Fe, Mn and Cu. However, there is a lack of uniformity between the representatives of the cestodes that have been studied (McCullough and Fairweather, 1987; von Brand et al., 1960; Scott et al., 1962; von Brand et al., 1965a). It was also observed that for the same species, the composition of the CCs varies according to their geographical origin (von Brand et al., 1965b). In this sense, it is argued that environment of the parasite, which depends directly from the host, influences the mineral composition (Etges and Marinakis, 1991).

Furthermore, concerning the structure of CC in cestodes, the existence of an organic fraction has been established (Smith and Richards, 1993; Vargas-Parada and Laclette, 1999), but the macromolecules and their roles in the biomineralization process have not been characterized to date.

The mineralized deposit of the cestode *Mesocestoides corti* in particular, has received attention and von Brand et al. (1965a) described the extraction of a calcium carbonate and magnesium compound that could not be identified. More recently, X-ray diffraction studies showed that the deposited mineral consists of

Abbreviations: CC, calcareous corpuscles; ACC, amorphous calcium carbonate; SEM, scanning electron microscopy; AFM, atomic force microscopy; XANES, -ray absorption near edge structure.

* Corresponding author. Tel.: +33 0 1 6915 6117; fax: +33 0 1 6915 6123.
E-mail address: yannicke.dauphin@upmc.fr (Y. Dauphin).

0968-4328/$ – see front matter © 2012 Elsevier Ltd. All rights reserved.
http://dx.doi.org/10.1016/j.micron.2012.06.008

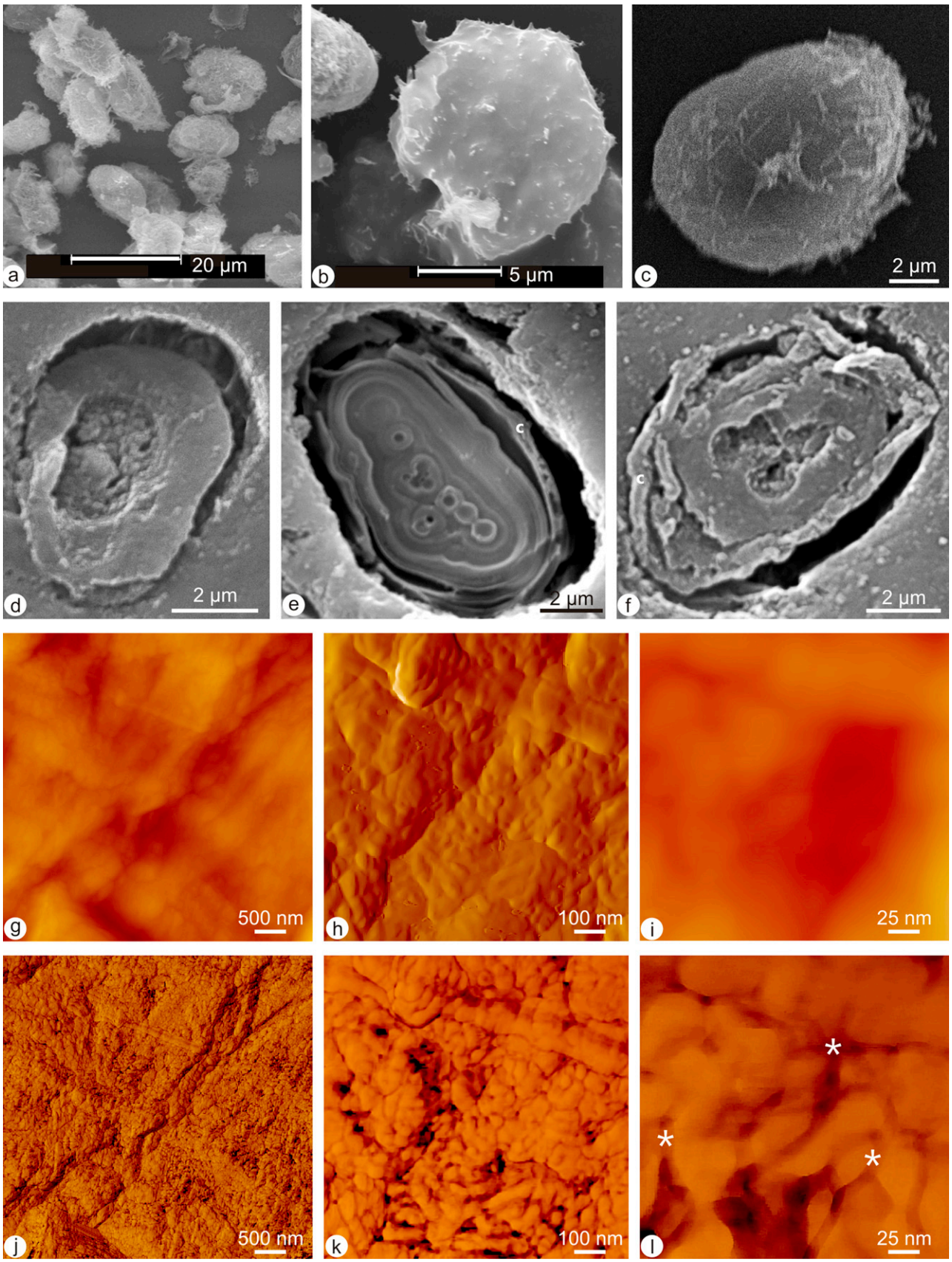

Fig. 1. Micro- and nanostructure of the calcareous corpsucles. (a) Dried corspuscles, showing the irregular shape and ornamented surface. SEM image. (b) Detail of a small round shape corpuscle with a smooth surface. Air dried sample. SEM image. (c) Detail of a small corpuscle with an ornamented surface. Air dried sample. SEM images. (d–f) Polished and etched sections showing the variable inner structure, with concentric layers and a more or less complex core. SEM images. (g) Polished section, showing no distinct topographical structure. Ultrasonication in H_2O–AFM height image. h- detail of the same sample. AFM amplitude image amplifies topographical details. (i) Detail of the same sample. At this scale of observation, AFM height image only shows indistinct features. (j) AFM phase image of (g). The heterogeneity and granular structure of the corpuscles are visible. (k) AFM phase image of (h). Cortex surrounding the granules is now visible. (l) AFM phase image of (i), showing the cortex around the granules (stars).

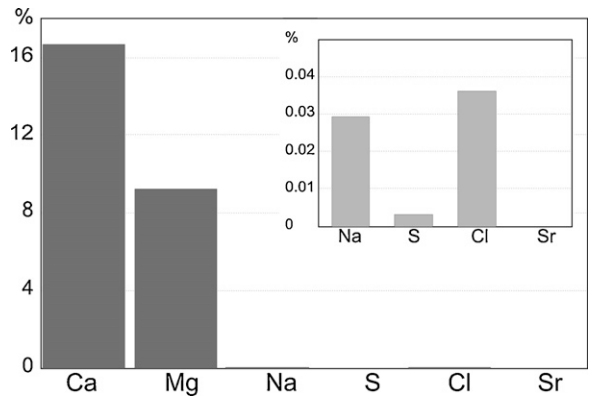

Fig. 2. Electron probe quantitative analyses of minor and major elements. Insert: detail of minor elements.

monohydrocalcite and amorphous calcium carbonate (ACC). FTIR analyses have confirmed the mineralogy, and showed the presence of an organic matrix (Señorale-Pose et al., 2008).

Since the knowledge of the structure and composition of CC is relevant for understanding the mechanisms involved in mineralization process and to determine their biological role, our aim was to characterize more precisely the structure of the CC of *M. corti*. In the present work, we analyzed the structure of CC employing a variety of technical approaches including Scanning electron microscope (SEM), Atomic force microscopy (AFM), Wavelength dispersive microprobe (WDS) and X-ray Absorption Near Edge Structure (XANES).

2. Materials and methods

2.1. Parasites – isolation of calcareous corpuscles

Calcareous corpuscles of *M. corti* were obtained from tetrathyridium larvae, as previously described (Señorale-Pose et al., 2008).

2.2. Embedding and polishing

Samples were embedded in resin, polished using various grades of diamond pastes down to a final 0.25 mm grade. Samples were then cleaned with a detergent mixed with hot water for 1 min under ultrasonication to remove any oil residue, and rinsed with tap water. Then, according to the technique subsequently employed, additional preparative procedures were undertaken, the details of which are given below in the related methods.

2.3. Scanning electronic microscopy

Air-dried samples and sections have been observed using a Philips XL30 SEM (Geosciences, Université Paris Sud). Diamond paste polished sections were etched with a solution of 5% H_3PO_4 for 2 s at room temperature. They were then rinsed with Milli-Q water and air dried at room temperature.

2.4. Atomic force microscopy (AFM)

Samples were studied using a Nanoscope IIIa multi-mode scanning probe microscope operating in tapping mode alone, or with the phase imaging extension (Geosciences, Université Paris Sud). The tapping mode AFM utilizes an oscillating tip at tip amplitude of approximately several tens of nm when the tip is not in contact with the surface. The resolution of tapping mode AFM is in the order of a few nanometers; no sample coating is necessary and observations were carried out in air.

2.5. Wavelength dispersive spectrometry (WDS)

Wavelength-dispersive X-ray microanalysis was used to analyze CC samples using a Cameca SX50 electron microprobe at the Natural History Museum (London). For quantitative analysis, the operating conditions were 15 kV accelerating voltage, 20 nA specimen current with a defocused beam. For maps, a 100 nA specimen current was used. Samples were coated with a thin carbon coat to ensure a good conductivity.

2.6. X-ray absorption near-edge structure spectroscopy (XANES)

This study was carried out at the X-ray Microscopy Beamline ID21 of the European Synchrotron Radiation Facility (ESRF, Grenoble, France). The X-ray beam energy was tuned around the sulphur K-edge (2472 eV) using a fixed exit double crystal Si(1 1 1) monochromator, providing an energy resolution of $\Delta E/E = 10^{-4}$ necessary to resolve the XANES features. In the scanning X-ray microscope (SXM), a germanium Fresnel zone plate optimized for this energy range was used to focus the beam to a submicron microprobe. The photon flux in the X-ray microprobe within the bandwidth of the double crystal Si(1 1 1) monochromator was 4×10^8 photons s^{-1}. A high purity Ge energy dispersive detector (Princeton Gamma-Tech, NJ) mounted in the horizontal plane perpendicular to the beam was used to collect the fluorescence photons emitted from the sample. The monitoring of the incoming beam intensity on the sample, which is essential to correct the acquired XANES spectra and images for beam intensity fluctuations, was ensured using a drilled photo-diode collecting the fluorescence from a 0.75 μm thick Al foil inserted in the beam path. The SXM was operated under vacuum to avoid the strong absorption of the sulphur emission lines by air. Although the primary beam energy was set around that of the S K-edge energy region, elements with absorption edges at lower energies were also subject to excitation and emission of fluorescence photons, and could therefore be determined. Thus, microfluorescence element maps of Mg and P were obtained simultaneously with the S maps. Reference spectra of standard compounds (S containing amino acids, chondroitin sulphate) were acquired for energy calibration in unfocussed mode (i.e., without the zone plate but with a 200 μm aperture defining the beam size). For these concentrated standards, the HpGe detector was replaced by a Si photodiode for the fluorescence signal measurements. Standards were finely grounded and deposited between two ultralene foils. Energy scans between 2450 eV and 2540 eV were performed with 0.225 eV increments.

3. Results

3.1. Structure

Calcareous corpuscles were first examined by SEM. They appear as irregular round or ovoid granules, variable in shape and size, in the range of 5–15 micrometers in diameter (Fig. 1a–c). Their outer surface is more or less smooth, but does not show a regular structural pattern.

Sections show various internal structures (Fig. 1d–f). A more or less thick outer cortex is visible. In some samples, this cortex is composed of several thin layers (Fig. 1e). Despite the samples being mounted in epoxy resin, the cortex does not stick to the inner layers. The core of the CC is empty in most cases (Fig. 1d and f), but some samples show a complex structure of multiple spheroids (Fig. 1e). Each spheroid is also composed of a cortex and a less acid resistant core.

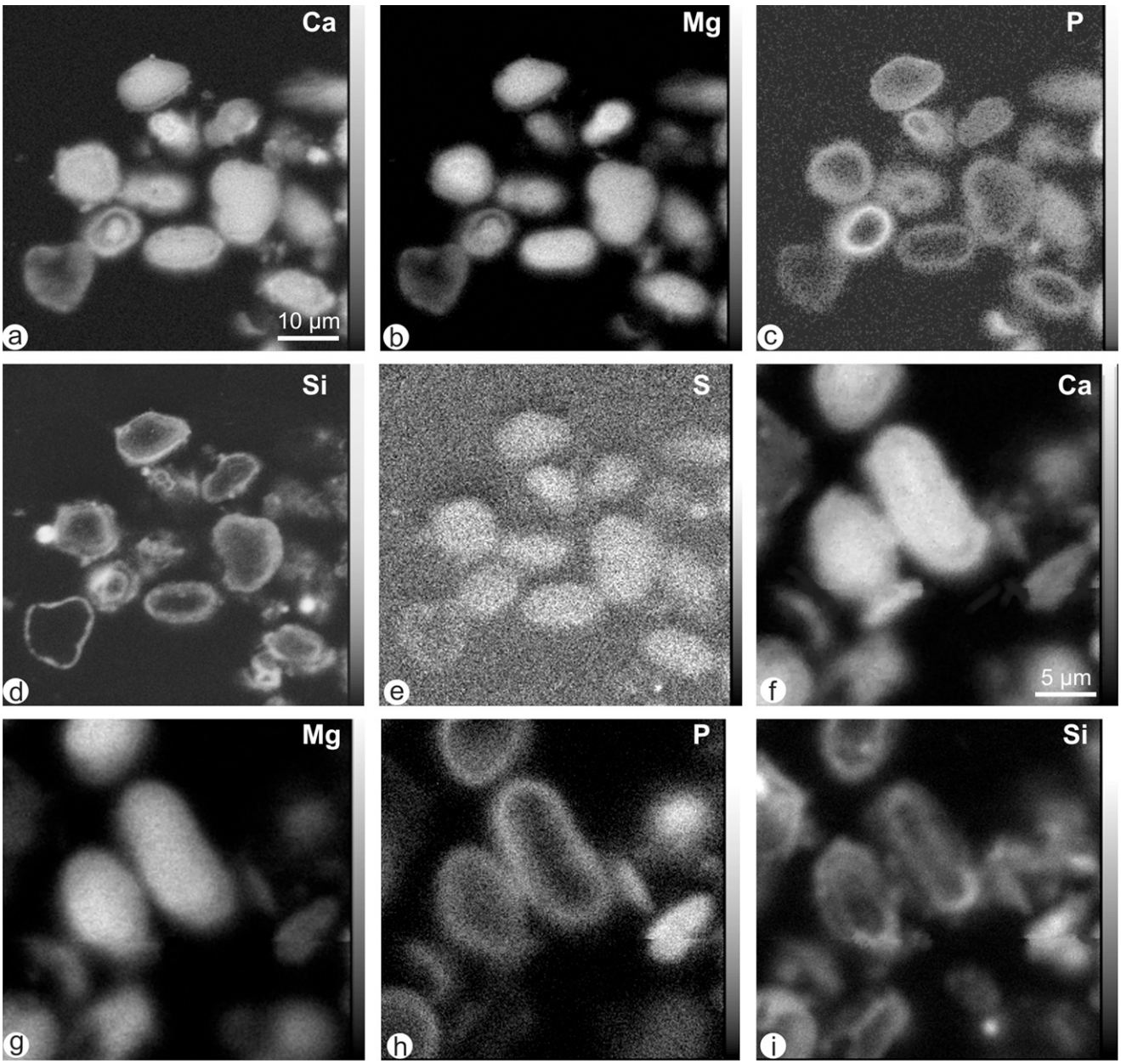

Fig. 3. Electron microprobe distribution maps; white is indicative of a high content (color scale on the right part of image).

The different parts of the CC are not homogeneous. Although AFM height images do not resolve nanostructural features (Fig. 1g and i), phase and amplitude images, sensitive to the composition and hardness, show inner irregular arrangements of granules (Fig. 1h and j–l). The shapes of the granules are irregular, but they are surrounded by a cortex observed in phase images (Fig. 1k and l). This cortex is not visible in height image (Fig. 1j). The thickness of the cortex is about ~8 nm. From what is known about the composition of corpuscles and the properties of phase images, it can be suggested that the composition of the cortex is different from that of the inner part of the granules.

3.2. Composition

Because of the fragility of samples (they decompose under the beam of the electron microprobe), only 3 punctual wavelength-dispersive X-ray quantitative microanalyses have been made. Average values are given in Fig. 2. Ca and Mg contents are high. From the matrix calculation made by the software of the microprobe, O content is high. Na, S, Cl contents are low and Sr is not detected. Two series of chemical maps were done at different places and with different magnifications (Fig. 3a–e, Fig. 3f–j). Ca, Mg, P and Si maps show the concentric layers in both general and detailed maps. The S map shows that corpuscles contain sulphur, but the layered organization is not visible (Fig. 3e).

The high spectral resolution around the sulphur K-edge obtained using the micro-XANES setup of ID21 at ESRF enables different chemical states of sulphur to be mapped based on minor differences in energy levels. Amino acids (cystine, cysteine and methionine), calcium sulphate and chondroitin sulphate were used as standards, and the energy positions of the peaks for each of these standards were determined before analyses of biominerals. Cystine, with a disulphide bond, displays a characteristic double peak at 2.4727 keV (Fig. 4A). Methionine and cysteine have no disulphide bond (Fig. 4A). Their S K-edge spectra have a main peak near 2.473 keV (Fig. 4A). The mineral sulphate ($CaSO_4$) and the sugar

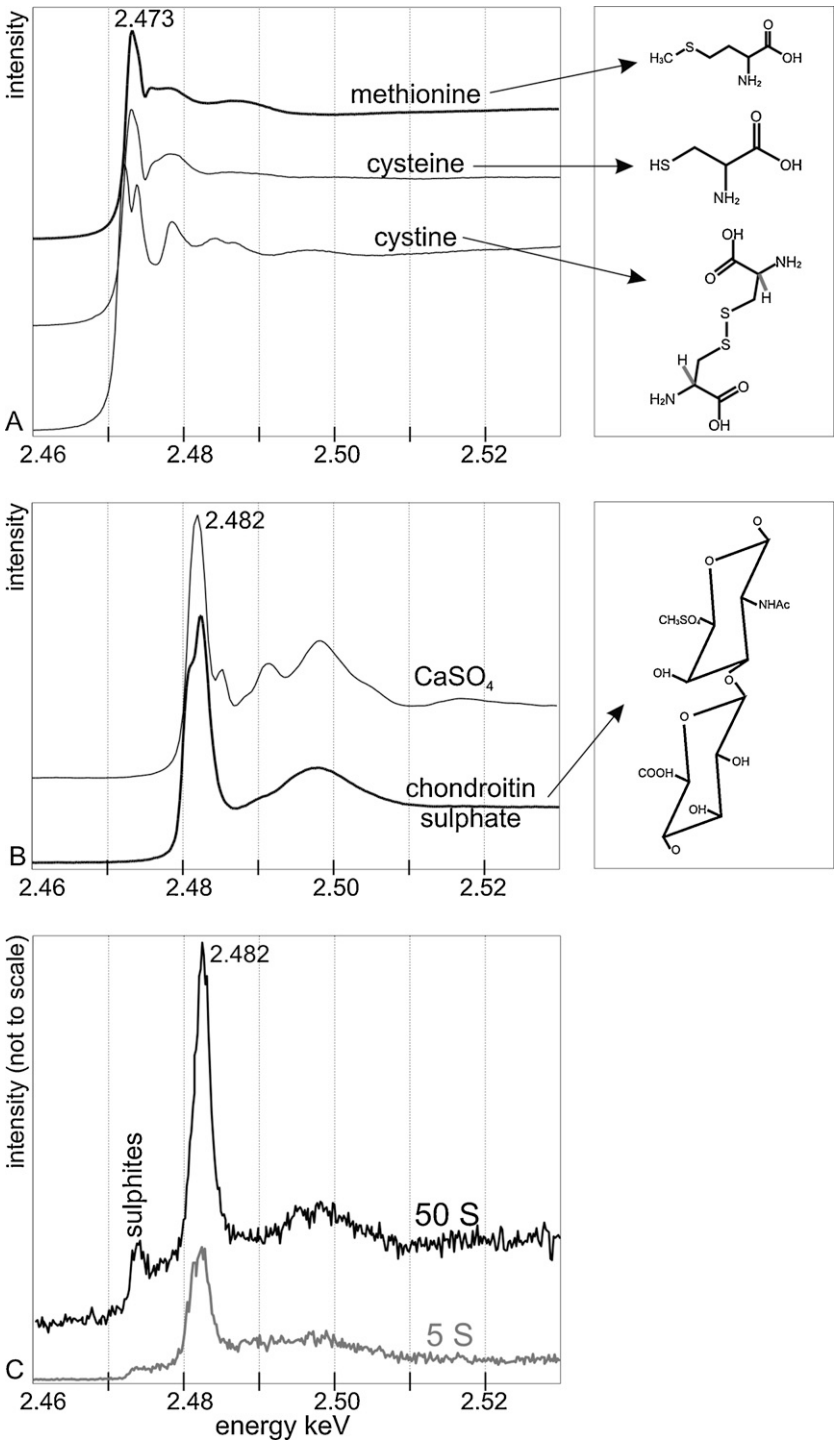

Fig. 4. XANES spectra. (A) S aminoacids, (B) organic (chondroitin sulphate) and mineral sulphates, (C) *Mesocestoides corti*.

chondroitin sulphate both have main peaks at 2.4827 keV (Fig. 4B). However, chondroitin sulphate has a shoulder in the ascendant (higher energy) slope of the main peak, whereas $CaSO_4$ has a shoulder in the descendant (lower energy) part of the main peak, as well as several additional structures at energies above 2.485 keV.

XANES spectra show the presence of sulphur in the CC of *Mesocestoides* (Fig. 4C). Comparison with standards shows that sulphur associated with amino acids in proteins is very low or absent, whereas organic sulphate content is high. However, under the beam, samples become modified. In the first spectra, sulphites are absent (Fig. 4C: 5 S), but the peak increases during the acquisition (Fig. 4C:50 S). Corpuscles are unstable under the beam, so that only short time acquisition maps were possible. However, these maps display the presence of organic sulphate, Mg and P (Fig. 5).

4. Discussion

The calcareous corpuscles of *Mesocestoides corti* are mineralized, and composed of an unusual mixture of hydrated $CaCO_3$, monohydrocalcite ($CaCO_3$, H_2O), and amorphous calcium carbonate (ACC). As for other calcareous biominerals, they also contain organic matrices (Señorale-Pose et al., 2008).

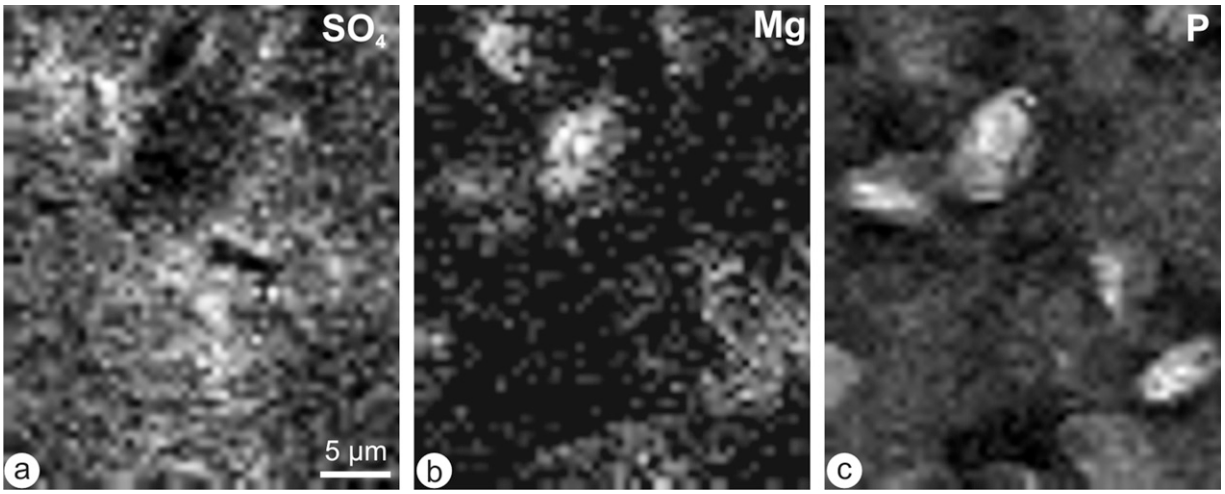

Fig. 5. XANES maps of *Mesocestoides corti*. (A) organic sulphate, (B) magnesium, (C) phosphorus.

4.1. Structure and composition of M. corti corpuscles

The size of the CCs (5–15 μm), as well as their outer ornamentation, is irregular. The inner structure is not dense, and composed of several layers, the number of which varies. The core structure is also variable. In some cases, tiny concretions with structural characteristics similar to the whole CC can be perceived in SEM images, reminiscent of a fractal structure. This is consistent with previous reports, which state that the *M. corti* CCs have originated by the coalescence of "immature" smaller CCs (Hess, 1980). The layers are granular composite structures, as shown by AFM phase images. The constituents of this material are irregular granules of about 30–100 nm, which are surrounded by a cortex of about 8 nm. A similar layered pattern was observed by TEM in the CCs of *Echinococcus granulosus* (Smith and Richards, 1993). These patterns could be the result of a cyclic process of biomineral deposition in cestodes.

The main elemental components are Ca and O. Mg content is high, whereas Na, S, Cl and Sr contents are low, which is consistent with previous reports (von Brand et al., 1960, 1965a,b; Etges and Marinakis, 1991). P, S and Si are also present. However, topological composition shows that Si and P are more abundant in the outer layer of the CCs. In contrast, Mg content is lower in the cortex of the CC in these qualitative maps. S is present in the form of organic sulphate, and no layered distribution is observed. In $CaCO_3$ mollusc shells and coral skeletons, it has been shown that organic sulphate is in the form of acidic sulphated polysaccharides (Cuif et al., 2003; Dauphin, 2003; Dauphin et al., 2003a,b). In calcitic brachiopod shells, organic sulphate is the dominant component, despite a very small fraction being present in the carbonate part (Cusack et al., 2008).

4.2. Comparison with other biogenic "concretions"

As previously shown by Señorale-Pose et al. (2008), the CCs of *M. corti* are rich in ACC and monohydrocalcite. Few organisms are able to synthesize a mixture of hydrated $CaCO_3$, monohydrocalcite and ACC. ACC is a metastable phase, but various organisms produce stable rich Mg ACC (Chave, 1954a,b; Bischoff et al., 1987). Intracellular mineralized granules have been found in the soft tissues of gastropods (Mason and Nott, 1981) and the composition of these granules depends on the taxa and environment, as they play a role in detoxification processes.

More recently, ACC has been detected as a precursor for crystalline structures in various taxa (Aizenberg et al., 2002; Beniash et al., 1997; Weiss et al., 2002). The storage concretions of *Orchestia cavimana*, a terrestrial Amphipod (Crustacea) contain ACC and amorphous calcium phosphate (Raz et al., 2002). Another Crustacea (*Porcellio*) secretes sternal deposits composed of small spheres (from 2 to 500 nm diameter). The spheres comprise concentric layers, composed of globular granules (10–40 nm in diameter), and organic filaments. These deposits were composed of amorphous Ca carbonate, and the size of amorphous particles varies from 10 to 30 nm (Becker et al., 2003). Amorphous granules with concentric layers were also observed in the hepatopancreas of a crab. These granules are rich in Ca phosphate and glucose 6-phosphatase (Corrêa et al., 2009). Our chemical maps show that Ca, P and Mg are co-localized in the concentric layers of the granules.

ACC precipitation *in vitro* used additives, among them molecules containing phosphate and or Mg. Ca carbonate monohydrate is synthesized using additives such as polyphosphate and Mg (Brooks et al., 1950). The *in vitro* stabilising role of Mg has been confirmed by Loste et al. (2003). According to Lam et al. (2007) "there is a direct correlation between the quantity of Mg contained within Mg–ACC with that in the post-crystallisation magnesian-calcite product". More surprising, *in vitro* experiments showed that depending on silica concentration, ACC is temporarily or permanently stable, or allowed to coexist with calcite (Kellermeier et al., 2010). The nanoparticles obtained in these *in vitro* experiments have a shape and size similar to those found in *Mesocestoides* CCs. Moreover, the *in vitro* formed nanoparticles are coated with an "outer skin" the thickness of which is about 9 nm, composed of hydrated amorphous silica. Even if this feature observed by Kellermeier et al. (2010), is similar to that observed in this work, the cortical composition of the granules that form the CCs is still unknown. The possible role of Si in the first stage of calcareous biomineralization has been evidenced in crustacean cuticle and bacterial induced calcite (Matsko et al., 2011). However, the role of organic matrix, Mg or Si in the stabilization of ACC in *Mesocestoides* CCs remains an open question.

ACC is also present in some plants as cystoliths. From the comparison of the chemical contents of two species, Gal et al. (2010) have shown that Si stabilizes ACC.

4.3. What is ACC?

ACC is the abbreviation for amorphous calcium carbonate. ACC is common in invertebrate skeletons, and is usually said to be a "precursor" for a more stable $CaCO_3$ polymorph. However, this explanation is not so simple. In the biominerals (spicules of an ascidian, lobster carapace and cystoliths) ACC exists but their structures differ. These ACC have the stochiometry of monohydrocalcite,

a trigonal rhombohedric mineral (Levi-Kalisman et al., 2000, 2002). These authors have also noticed that the ACC behaves differently when extracted from the organism. ACC from cystoliths become calcite when air dried, whereas ACC from ascidian spicule and lobster do not change. This behavior emphasizes the diversity of observations on ACC stability. From the comparison of biogenic and *in vitro* minerals, Neumann and Epple (2007) concluded that "nanoscopic particles of hydrated calcium carbonate (resembling monohydrocalcite) assemble into water-containing ACC but do not crystallise (as shown by the fact that biogenic ACC is X-ray-amorphous), which means that the aggregates possess a higher energy than crystalline monohydrocalcite".

Up to now, the role of the corpuscles is still unknown. Rounded granules with concentric structures have been described in the shell repair membrane in mollusc (Abolins-Krogis, 1973). Ca carbonate is present as ACC or shows a weak X-ray diffraction. Histochemical stainings have shown that these granules are also biocomposites, with lipids, proteins and glycosaminoglycans.

5. Conclusion

The biomineral concretions found in *Mesocestoides corti* known as calcareous corpuscles are spheroid or ovoid layered structures (5–15 μm). Layers are composite structures constituted by granules of tens of nm, each surrounded by a cortex of about 8 nm. Such an arrangment is found in the most calcareous skeletons: fish otoliths (Dauphin and Dufour, 2008), sponges (Cuif et al., 2011), corals (Cuif and Dauphin, 2005; Farre et al., 2010) and molluscs (Dauphin, 2001; Dauphin et al., 2003a,b). Several factors could stabilize the amorphous calcium carbonate in this kind of particles, including organic molecules, as well as Si, Mg and P, all of them present in the CCs. Despite the similarities with granules observed in other organisms (Molluscs), a repairing role of the *Mesocestoides* granules is not an option. Another common hypothesis is a detoxification or waste storage (Simkiss, 1977; Vargas-Parada and Laclette, 1999). The complex chemical composition of the granules is not inconsistent with such roles.

Acknowledgements

The authors wish to thank Dr. L. Dominguez and Dr. J. Saldaña (Facultad de Química, Universidad de la República, Uruguay) for the donation of *M. corti* tetrathyridia. This work was supported by PEDECIBA (Uruguay), and grants from ESRF (EC 24) and SYNTHESIS program (GB-TAF 3612).

References

Abolins-Krogis, A., 1973. Fluoprescence and histochemical studies of the calcification-initiating lipofuscin type pigment granules in the shell-repair membrane of the snail, *Helix pomatia* L. Zeitschrift fur Zellforschung und Mikroskopische Anatomie 142, 205–221.

Aizenberg, J., Lambert, G., Weiner, S., Addadi, L., 2002. Factors involved in the formation of amorphous and crystalline calcium carbonate: a study of an ascidian skeleton. Journal of the American Chemical Society 124 (1), 32–39.

Becker, A., Bismayer, U., Epple, M., Fabritius, H., Hasse, B., Shi, J., Ziegler, A., 2003. Structural characterization of X-ray amorphous calcium carbonate (ACC) in sternal deposits of the crustacea Porcellio scaber. Dalton Transactions, 551–555, http://dx.doi.org/10.1039/b210529b.

Beniash, E., Aizenberg, J., Addadi, L., Weiner, S., 1997. Amorphous calcium carbonate transforms into calcite during sea urchin larval spicule growth. Proceedings of the Royal Society B 264, 461–465.

Bischoff, W.D., Mackenzie, F.T., Bishop, F.C., 1987. Stabilities of synthetic magnesian calcites in aqueous solution: comparison with biogenic materials. Geochimica et Cosmochimica Acta 51, 1413–1423.

Brooks, R., Clark, L.M., Thurston, E.F., 1950. Calcium carbonate and its hydrates. Philosophical Transactions of the Royal Society of London Series A 243, 145–167.

Chave, K.E., 1954a. Aspects of the biogeochemistry of magnesium. 2. Calcareous sediments and rocks. Journal of Geoleogy 62, 587–599.

Chave, K.E., 1954b. Aspects of the biogeochemistry of magnesium. 1. Calcareous marine organisms. Journal of Geoleogy 62, 266–283.

Corrêa Jr., J.D., Bruno, M.I., Allodi, S., Farina, M., 2009. Effects of H^+ concentration on amorphous mineral granules: Structural stability and elemental mobilization. Journal of Structural Biology 166, 59–66.

Cuif, J.P., Dauphin, Y., 2005. The environmental recording unit in coral skeletons – a synthesis of structural and chemical evidences for a biochemically driven, stepping-growth process in fibres. Biogeosciences 2, 61–73.

Cuif, J.P., Dauphin, Y., Doucet, J., Salomé, M., Susini, J., 2003. XANES mapping of organic sulfate in three scleractinian coral skeletons. Geochimica et Cosmochimica Acta 67, 75–83.

Cuif, J.P., Dauphin, Y., Sorauf, J.E., 2011. Biominerals and Fossils Through Time. Cambridge Univ. Press, Cambridge.

Cusack, M., Dauphin, Y., Cuif, J.P., Salomé, M., Freer, A., Yin, H., 2008. Micro-XANES mapping of sulphur and its association with magnesium and phosphorus in the shell of the brachiopod, *Terebratulina retusa*. Chemical Geology 253, 172–179.

Dauphin, Y., 2001. Nanostructures de la nacre des tests de céphalopodes actuels. Paläontologische Zeitschrift 75, 113–122.

Dauphin, Y., 2003. Soluble organic matrices of the calcitic prismatic shell layers of two pteriomorphid Bivalves: *Pinna nobilis* and *Pinctada margaritifera*. Journal of Biological Chemistry 278, 15168–15177.

Dauphin, Y., Cuif, J.P., Doucet, J., Salomé, M., Susini, J., Williams, C.T., 2003a. In situ chemical speciation of sulfur in calcitic biominerals and the simple prism concept. Journal of Structural Biology 142, 272–280.

Dauphin, Y., Dufour, E., 2008. Nanostructures of the aragonitic otolith of cod (*Gadus morhua*). Micron 39, 891–896.

Dauphin, Y., Guzman, N., Denis, A., Cuif, J.P., Ortlieb, L., 2003b. Microstructure, nanostructure and composition of the shell of *Concholepas concholepas* (Gastropoda, Muricidae). Aquatic Living Resources 16, 95–103.

Etges, F.J., Marinakis, V., 1991. Formation and excretion of calcareous bodies by the metacestode (Tetrathyridium) of *Mesocestoides vogae*. Journal of Parasitology 77, 595–602.

Farre, B., Cuif, J.P., Dauphin, Y., 2010. Occurrence and diversity of lipids in modern coral skeletons. Zoology 113, 250–257.

Gal, A., Weiner, S., Addadi, L., 2010. The stabilizing effect of silicate on biogenic and synthetic amorphous calcium carbonate. Journal of the American Chemical Society 132, 13208–13211.

Hess, E., 1980. Ultrastructural study of the tetrathyridium of *Mesocestoides corti* Hoeppli, 1925: tegument and parenchyma. Zeitschrift fur Parasitenkunde 61, 135–159.

Kellermeier, M., Melero-Garcia, E., Glaab, F., Klein, R., Drechsler, M., Rachel, R., Garcia-Ruiz, J.M., Kunz, W., 2010. Stabilization of amorphous calcium carbonate in inorganic silica-rich environments. Journal of the American Chemical Society 132, 17859–17866.

Lam, R.E.K., Charnock, J.M., Lennie, A., Meldrum, F.C., 2007. Synthesis – dependant structural variations in amorphous calcium carbonate. CrystEngComm 12, 1226–1236.

Levi-Kalisman, Y., Raz, S., Weiner, S., Addadi, L., Sagi, I., 2000. X-ray absorption spectroscopy studies on the structure of a biogenic amorphous calcium carbonate phase. Journal of the Chemical Society – Dalton Transactions, 3977–3982.

Levi-Kalisman, Y., Raz, S., Weiner, S., Addadi, L., Sagi, I., 2002. Structural differences between biogenic amorphous calcium carbonate phases using X-ray absorption spectroscopy. Advanced Functional Materials 12, 43–48.

Loste, E., Wilson, R.M., Seshadri, R., Meldrum, F.C., 2003. The role of magnesium in stabilising amorphous calcium carbonate and controlling calcite morphology. Journal of Crystal Growth 254, 206–218.

Lowenstam, H.A., 1981. Minerals formed by organisms. Science 211, 1126–1131.

McCullough, J.S., Fairweather, I., 1987. The structure, composition, formation and possible functions of calcareous corpuscles in *Trilocularia acanthiaevulgaris* Olsson 1867 (Cestoda Tetraphyllidea). Parasitology Research 74, 175–182.

Mason, A.Z., Nott, J.A., 1981. The role of intracellular biomineralized granules in the regulation and detoxification of metals in gastropods with special reference to the marine prosobranch Littorina littorea. Aquatic Toxicology 1, 239–256.

Matsko, N.B., Znidarsic, N., Letofsky-Papst, I., Dittrich, M., Grogger, W., Strus, J., Hofer, F., 2011. Silicon: The key element in early stages of biocalcification. Journal of Structural Biology 174, 180–186.

Neumann, M., Epple, M., 2007. Monohydrocalcite and its relationship to hydrated amorphous calcium carbonate in biominerals. European Journal of Inorganic Chemistry, 1953–1957.

Raz, S., Testenière, O., Hecker, A., Weiner, S., Luquet, G., 2002. Stable amorphous calcium carbonate is the main component of the calcium storage structures of the crustacean *Orchestia cavimana*. Biological Bulletin 203, 269–274.

Scott, D.B., Nylen, M.U., von Brand, T., Pugh, M.H., 1962. The mineralogical composition of the calcareous corpuscle of *Taenia taenieformis*. Experimental Parasitology 12, 445–458.

Señorale-Pose, M., Chalar, C., Dauphin, Y., Massard, P., Pradel, P., Marín, M., 2008. Monohydrocalcite in calcareous corpuscles of *Mesocestoides corti*. Experimental Parasitology 118, 54–58.

Simkiss, K., 1977. Biomineralization and detoxification. Calcified Tissue Research 24, 199–200.

Smith, S.A., Richards, K.S., 1993. Ultrastructure and microanalyses of the calcareous corpuscles of the protoscoleces of *Echinococcus granulosus*. Parasitology Research 79, 245–250.

Smyth, J.D., 1969. The Physiology of Cestodes. WH Freeman & Company, San Francisco, California.

Vargas-Parada, L., Laclette, J.P., 1999. Role of the calcareous corpuscles in cestode physiology: a review. Revista Latinoamericana de Microbiologia 41, 303–307.

von Brand, T., Mercado, T.I., Nylen, M.U., Scott, D.B., 1960. Observations on function, composition, and structure of cestode calcareous corpuscles. Experimental Parasitology 9, 205–214.

von Brand, T., Scott, D.B., Nylen, M.U., Pugh, M.H., 1965a. Variations in the mineralogical composition of cestode calcareous corpuscles. Experimental Parasitology 16, 382–391.

von Brand, T., Nylen, M.U., Scott, D.B., Martin, G.N., 1965b. Observations on calcareous corpuscles of larval *Echinococcus granulosus* of various geographic origins. Proceedings of the Society for Experimental Biology and Medicine 120, 383–385.

Weiss, I.M., Tuross, N., Addadi, L., Weiner, S., 2002. Mollusc larval shell formation: amorphous calcium carbonate is a precursor phase for aragonite. Journal of Experimental Zoology 293, 478–491.

Wilt, F.H., Killian, C.E., Livingston, B.T., 2003. Development of calcareous skeletal elements in invertebrates. Differentiation 71, 237–250.